

## BENDING STRENGTH OF LAYERED FIBERCONCRETE PRISMS

**Vitalijs Lusis\***

\*Riga Technical University  
Concrete mechanics laboratory  
E-mail: [Vitalijs.Lusis@rtu.lv](mailto:Vitalijs.Lusis@rtu.lv)

**Andrejs Krasnikovs\*\***

\*\*Riga Technical University  
Institute of Mechanics and Concrete mechanics laboratory  
E-mail: [Krasnikovs.Andrejs@gmail.com](mailto:Krasnikovs.Andrejs@gmail.com)

### ABSTRACT

*Fiber reinforced concrete is an important material for structural applications. Traditionally fibers are homogeneously dispersed in concrete volume. At the same time in many situations material with homogeneously dispersed fibers is not optimal (the majority of added fibers are not participating in the load bearing process). In the present research fiber reinforced concrete prisms with layers contained different fibers concentrations inside them were elaborated. Prisms were tested under four point bending conditions, experimental results were discussed.*

**Key words:** fiber concrete, layered structure, numerical modelling

### INTRODUCTION

While in most of the currently available design recommendations fiber reinforced concrete strength properties are observed using the inverse approach (approximating the experimentally obtained curve), it should be noted that the direct modelling approach allows one to perform an economically optimal design of fiber reinforced concrete structure and to obtain the characterization of fibers distribution and their spatial orientations in structural element volume (Krasnikovs A. et al., 2008; Krasnikovs A. et al., 2009; Krasnikovs A. et al., 2012; Li V. C., 2003). In the present research three different types of layered prisms with the same amount of fibers in them were experimentally produced, three samples with the dimensions of 100×100×400 mm were created for each type and four prisms with homogeneously dispersed fibers were produced for reference as well. Prisms were tested under four point bending conditions until crack openings in each prism reached 6 mm. Simultaneously, prism cracking was simulated numerically using an elaborated numerical model for neutral axes location in the prism during crack growth and cracked beam load bearing capacity during crack growth and opening. The numerical modelling results were compared with the experimentally obtained ones. Finally, conclusions about fracture process features were made.

### EXPERIMENTAL INVESTIGATION

In the framework of this research prisms of non-homogeneous fiber reinforced concrete with the dimensions 100×100×400 mm were designed. The technology of specimen preparation is described in the patent (Lapsa V. et al., 2011). Three identical

prisms of each type of non-homogeneous fiber reinforced concrete were prepared. Prisms were tested under four point bending conditions using the „CONTROLS” Automax 5 loading machine.

#### Specimens preparation

Groups of specimens are presented in the Table 1. Group 1 consists of fiber reinforced concrete with fibers homogeneously dispersed in the sample volume. These prisms were used as reference. As seen in Table 1, while the total amount of fibers is identical for all four groups of specimens, the difference is in their distribution. For specimens of Groups 2, 3 and 4, fibers are distributed in different layers with various concentration and orientation. These specimens can be defined as layered prisms with oriented distribution of fibers.

Steel end-hooked fibers Dramix RC 80/30 BP with the following parameters were used: length - 30 mm, fiber aspect ratio 80, and tensile strength 1020Mpa.

Fibers were added to the mix during the concrete mixing process and moulds were filled by such fiberconcrete for specimens representing Group 1 see in figure 1. For the specimens from Groups 2, 3, and 4, moulds were gradually filled with the concrete mix according to the description of each group. Then fibers were uniformly scattered on the concrete surface in the mould and were pressed into concrete (figure 2, 3 and 4).

**Table 1**  
Distribution and concentration of fibers in specimens

Group Nr.	Distribution and concentration of fibers
Group Nr.1.	Fibers mixed in concrete mixer and homogeneously dispersed in the specimen (classical method)
Group Nr.2.	1. 25mm of concrete – 1/2 of the total amount of fibers (60 kg/m <sup>3</sup> ) were pressed into concrete 2. 25mm of concrete – 1/2 of the total amount of fibers (60 kg/m <sup>3</sup> ) were pressed into concrete 3. 50mm of concrete without fibers
Group Nr.3.	1. 25 mm of concrete – 2/3 of the total amount of fibers (60 kg/m <sup>3</sup> ) were pressed into concrete 2. 50 mm of concrete – 1/3 of the total amount of fibers (60 kg/m <sup>3</sup> ) were pressed into concrete 3. 25mm of concrete without fibers
Group Nr.4.	1. 25 mm of concrete – 2/3 of the total amount of fibers (60 kg/m <sup>3</sup> ) were pressed into concrete 2. 75mm of concrete – 1/3 of the total amount of fibers (60 kg/m <sup>3</sup> ) were pressed into concrete

For the specimen from Group 2, the mould was filled with 25 mm layer of concrete mix, then fibers (1/2 of the total amount of fibers 60 kg/m<sup>3</sup>) were uniformly scattered on the concrete surface in the mould and were pressed into concrete. Fibers were pressed by a steel grid into the concrete in the full length of the prism according to the Latvian patent LV14257 technology.

Then the mould was filled with concrete mix up to 50 mm and the rest of fibers were uniformly scattered on the concrete surface in the mould and were pressed into concrete. Fibers were pressed by a steel grid. Finally, the mould was filled with concrete mix up to 100 mm.

Density of fiber reinforced concrete ranges from 2350 to 2400 kg/m<sup>3</sup> (2375 kg/m<sup>3</sup> in average) and according to the concrete compressive strength testing results it corresponds to the compressive strength class C70/85. All specimens, namely, fiber reinforced concrete prisms were tested under four point bending conditions using the „CONTROLS” testing machine (figure 5).

Figure 1

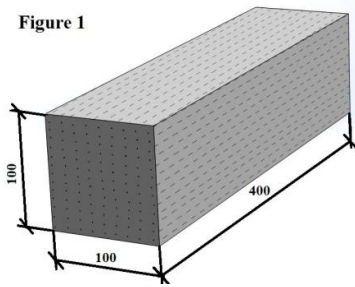


Figure 3

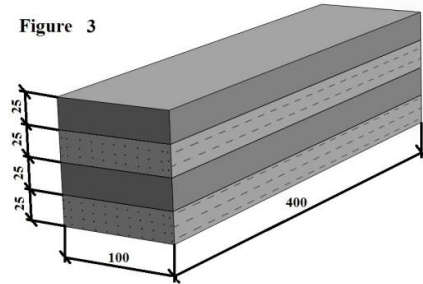


Figure 2

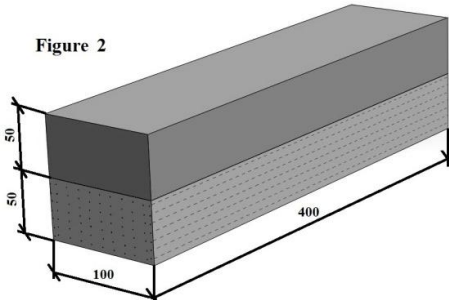


Figure 4

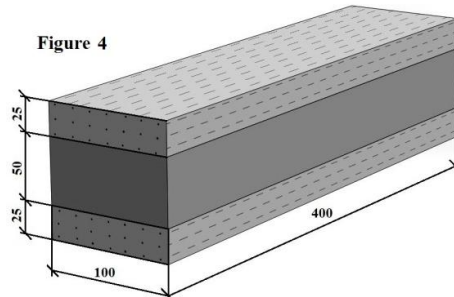


Figure 1; 2; 3; 4. Fibers distribution and concentration in samples



Figure 5. Testing device with fiber reinforced concrete prism

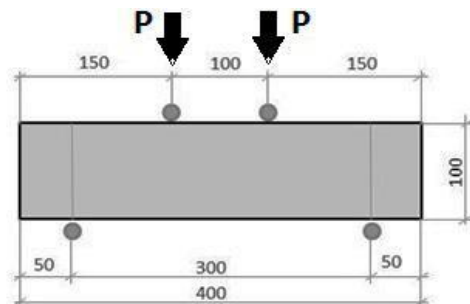


Figure 6. Picture of loads application to a fiber reinforced concrete beam

**Table 2**  
Concentrations of fibers in the layers of specimen

Group Nr.	Fiber dispersion in the height of prisms and concentration of fibers in specimens $\text{kg/m}^3$
Group Nr.1.	1. 100mm - 60 $\text{kg/m}^3$ . Fibers are homogeneously and chaotically dispersed in the volume of prism.
Group Nr.2.	1. 50mm – 120 $\text{kg/m}^3$ . Fibers are homogeneously and chaotically dispersed in the layer with thickness 50mm. 2. 50mm – concrete without fibers.
Group Nr.3.	1. 25mm – 160 $\text{kg/m}^3$ . Fibers are homogeneously and chaotically dispersed in the layer with thickness 25mm. 2. 25mm – concrete without fibers. 3. 25mm – 80 $\text{kg/m}^3$ . Fibers are homogeneously and chaotically dispersed in the layer with thickness 25mm. 4. 25mm – concrete without fibers.
Group Nr.4.	1. 25mm – 160 $\text{kg/m}^3$ . Fibers are homogeneously and chaotically dispersed in the layer with thickness 25mm. 2. 50mm – concrete without fibers. 3. 25mm – 80 $\text{kg/m}^3$ . Fibers are homogeneously and chaotically dispersed in the layer with thickness 25mm.

During testing, the vertical deflection at the centre of a prism and crack opening were fixed by the linear displacements transducers in real time. Sensors were connected through a data acquisition unit to the computer where the obtained data were recorded and were available after experiments.

### NUMERICAL MODELING

The computer modeling of fiber reinforced concrete cracking was performed using the previously developed numerical model (Krasnikovs A.et all., 2008; Krasnikovs A.et all., 2009; Krasnikovs A.et all., 2012). Assumptions regarding the fiber distribution in samples are shown in the Table 2.

### RESULTS AND DISCUSSION

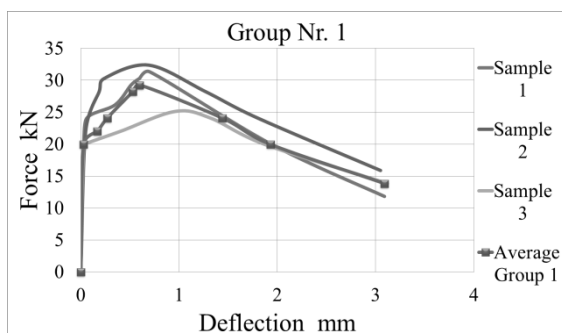


**Figure 7.** Load – sample centre vertical deflection graphs for specimens are representing group Nr.1

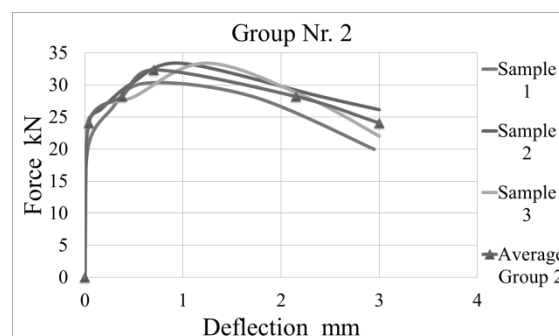


**Figure 8.** Load - sample centre vertical deflection graphs for specimens are representing group Nr.2

Specimens were tested under four point bending conditions. Load bearing - vertical deflection at the centre of each prism graphs for the specimens of Group 1 are given in figure 7.

The diagram shows the experimental curve of each specimen as well as the average value curve. Three stages are seen in each curve; first of them is linear elastic deflection (corresponds to deflection under 0,01mm). In this stage the fiber reinforced concrete prisms become deformed without visible crack openings.

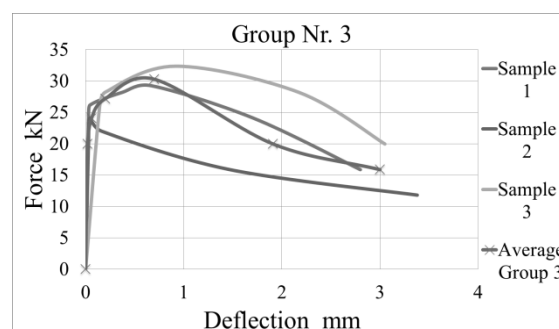


**Figure 9.** Load - sample centre vertical deflection graphs for specimens are representing group Nr.3

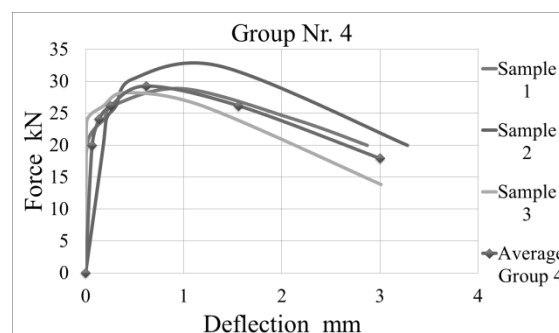


**Figure 10.** Load - sample centre vertical deflection graphs for specimens are representing group Nr.4

Fibers in the concrete do not bear significant load. The next stage begins with deviation of curves from the straight line and terminates reaching the maximum value on curve (with deflection of prisms 0,75mm – 1mm).

In this stage concrete micro cracks accumulate and grow forming a macro crack network. The macro cracks are formed perpendicularly to the longitudinal axis of prism. The density of the macro crack network depends on the specimen's geometry, size of fibers and their amount. Fibers traversing the macro cracks begin to bear load, while the cracks are still invisible on the outer surface of specimen.

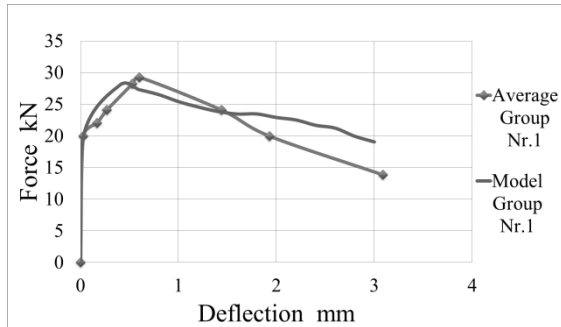


**Figure 11.** Load - sample centre vertical deflection graphs for specimens in Group Nr.1. The average result and modeling curve

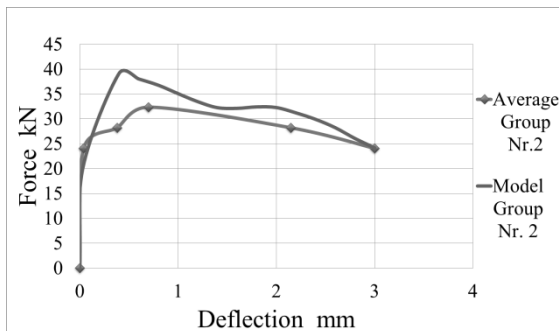


**Figure 12.** Load - sample centre vertical deflection graphs for specimens in Group Nr.2. The average result and modeling curve

The crack with the lowest resistance to opening (the one with the lower amount of fibers traversing it or fibers located and oriented in a less optimal way) starts to open. It proceeds the following way: fibers which are bearing load are delaminated from the concrete and start to pull out by one or both ends. The individual load carrying capacity of fiber depends on its orientation towards the crack plane and how far it is extracted.

Experimental observation of fiber pull-out micromechanics (Krasnikovs A.et all., 2009) showed that the maximum load carrying capacity of fiber depends on the orientation of fiber towards the direction of extraction force and how much the fiber has been extracted. The third stage is characterized by the decline of the total load carrying capacity of fiber. The capacity decreases proportionally to the size of the crack opening. Applied load - vertical deflection at the center of the prism for the specimens of Groups 2, 3 and 4 are given in figures 8, 9 and 10. Diagrams in figures 11, 12, 13 and 14 show the average experimental curves (from three

specimens) compared to the results of the numerical modeling. The modeling results approximate the data obtained experimentally in the first and second stage of curves. In the third stage the modeling results show a higher load carrying capacity for the specimens of Groups 1, 2 and 4 compared to the ones obtained experimentally.

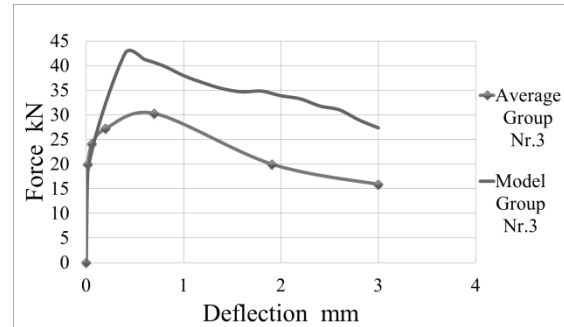


**Figure 13.** Load - sample centre vertical deflection graphs for specimens in Group Nr.3. The average result and modeling curve

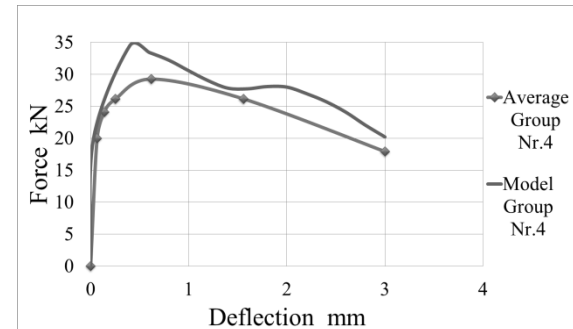


**Figure 14.** Load - sample centre vertical deflection graphs for specimens in Group Nr.4. The average result and modeling curve

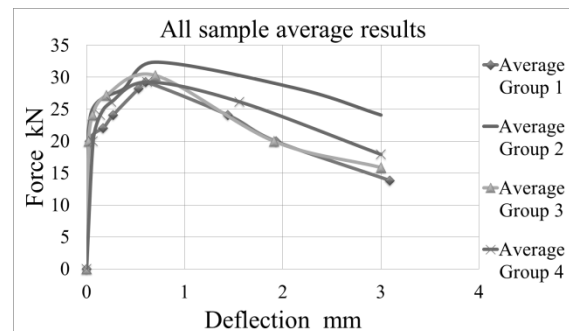


**Figure 15.** Load - sample centre vertical deflection graphs for specimens in comparison of average of all sample groups

The difference grows proportionally to the size of the crack opening. It can be explained by the homogenous distribution of fibers used in the model versus the non-homogenous in reality, for the specimens of Group 1, in the entire prism and for the specimens of Groups 2 and 4, in layers. Experimental (average) curves for all four groups are given in figure 15. It can be observed, that

Group 2 reaches the highest load carrying capacity during the crack opening stage due to the highest concentration of fibers compared to other groups in the lower part of the prism which bears the maximum tensile load. It can be observed, Group 1 (reference specimens) reaches lower average load carrying capacity in the third stage (macro cracks) compared to the specimens with the non-homogeneous distribution of fibers. Certain similar tendencies can be observed among the diagrams of the average results of the specimens – the maximal load carrying capacity is reached with deflection of prisms 0,75 mm – 1 mm, which correlates with the crack opening size.

## CONCLUSIONS

According to the testing results, specimens of Group 2 reached the highest load carrying capacity during the crack opening stage as they had the highest concentration of fibers in the part of prisms experiencing maximum tensile load. Specimens of Group 1 showed a lower average load carrying capacity during the crack forming stage compared to the specimens with the non-homogeneous distribution of fibers. The load carrying capacity of

the fiber reinforced concrete was compared with the numerical modelling. The modelling results approximate the data obtained experimentally in the first and second stage of curves. In the third stage (macro crack opening) the modelling results showed a higher load carrying capacity for the specimens of Groups 1, 2 and 4 compared to the ones obtained experimentally. The difference increases proportionally to the size of the crack opening. It can be explained by the assumption about homogenous distribution of fibers that were used in the model versus the non-homogenous in reality.

## ACKNOWLEDGMENT

This work has been supported by the European Social Fund within the project “Support for the implementation of doctoral studies at Riga Technical University”.



## REFERENCES

- Krasnikovs A., Kononova O. and Khabaz A. (2009) Fracture and Post-cracking Behavior Prediction for Glass and Carbon Fiber Reinforced Concrete Construction Members, Proceedings of 5th International Conference Fiber Concrete 2009 Technology, Design, Application, Prague p.161-166.
- Krasnikovs A., Kononova O. and Pupurs A. (2008) Steel Fiber Reinforced Concrete Strength. Sc. Proceedings of Riga Technical University. Transport and Engineering, 6, 28, p. 142-150.
- Krasnikovs A., Kononova O., Khabaz A., Machanovsky E. and Machanovsky A. (2012) Post-Cracking Behavior of High Strength (Nano Level Designed) Fiber Concrete Prediction and Validation. CD- Proceedings of 4th International Symposium on Nanotechnology in Construction, 20-22 May 2012, Crete, Greece, 6 p.
- Krasnikovs A., Kononova O. strength prediction for concrete reinforced by different length and shape short steel fibers// Sc. Proceedings of Riga Technical University. Transport and Engineering, 6, vol.31, p.89-93, 2009.
- Li V. C. (2003) On Engineered Cementitious Composites a Revue of the Material and it's Applications. Journal of Advanced Concrete Technology, Vol.1, No3, p. 215-230.
- Lapsa V., Krasnikovs A., Strauts K., (2011.20.04) „Fiberconcrete Non- Homogeneous Structure Element Building Technology Process and Equipment”, Latvian patent LV14257.